RESEARCH ON ELECTRON BEAM WELDING OF CR-MO STEELS

Daniel Drimal, Frantisek Kolenic, Tomas Fodrek, Rastislav Sekerka
PRVÁ ZVÁRAČSKÁ a. s., Kopcianska 14, Bratislava, 851 01, Slovakia

Abstract

The paper presents a comprehensive approach to the welding of CrMo hardenable steels. W. No. 1.7225 (42CrMo4) and W. No. 1.7325 (25MoCr4) using the advantages of electron beam technology. The experiments were carried out on a modified electron beam welding device of the PZ ELZA UNI 2G type with an acceleration voltage of up to 60 kV and a maximum power of up to 7 kW. The research was focused on the design and optimization of the preheating of welded parts to suppress the formation of cold cracks. Preheating was performed with a defocused and deflected electron beam before the actual welding process. Preheating parameters were designed based on theoretical calculations and verified in the process. The temperature of the weldment was monitored during preheating using a thermocouple, and the measured values were compared with the predicted ones. The achieved properties of the welded joints are presented in terms of the achieved structure and hardness.

Keywords: *electron beam welding, Cr-Mo steels, carbon equivalent, cold crack, preheating*

1. INTRODUCTION

Transmission mechanisms and gears are among the most highly stressed components. Compactness of design and material savings often require solutions made up of multiple components. The grinded gears can be spaced at a distance that prevents access of the grinding wheel. In that case, joining is the last operation. The material from which they are made also corresponds to the application conditions. Various types of carbon and low-alloy Cr-Mo, Cr-Mn steels are used as the structural material. These steels normally achieve tensile strengths above 1000 MPa and hardnesses above 56 HRC in the as-quenched condition. The increased C content and the presence of elements such as Cr and Mo, which improve the hardenability of the steel, result in the formation of hard and brittle structures at supercritical cooling rates what can deteriorate the weldablitlity. The chemical and microstructural composition also affects the weldability of these steels. Considering the tendency to form hard and brittle structural components, there is an assumption of an increased risk of cold cracks during welding. This must be taken into account when selecting the joining method. Brazed joints generally exhibit lower strength compared to welded joints and the effects of the brazing heat cycle may lead to annealing of the steel. Arc welding methods make and proper selection of filler material it allows to achieve the desired strength properties of welded joints. The disadvantage is the considerable thermal impact on the material accompanied by deformations. The optimum solution for joining such parts lies in the use of welding methods using concentrated energy sources such as laser and electron beam. Welds made with concentrated energy sources are characterized by the affectation of the material limited to the immediate vicinity of the weld, minimal deformation from welding, and allow welded joints to be made even in areas with difficult accessibility [1, 2, 3].

1.1. Analysis of the preheating by electron beam

One of the parameters defining the weldability of steel is its carbon equivalent (C_{eq}). It reflects the influence of the content of individual alloying elements in the steel on the increase of the hardness in weld metal (WM) and in the heat affected zone (HAZ) under welding process conditions. In general, steels with a carbon equivalent $C_{eq} \leq 0.45$ and a wall thickness of less than 20 mm are considered to have good weldability. Steels with a higher C_{eq} fall into the category of conditionally weldable and require special procedures to achieve a sound weld joint[4, 5, 6]. The calculation of the carbon equivalent recommended by the IIW for is given in eq. 1.

$$C_{eq} = C + \frac{Mn}{6} + \frac{Cr+Mo+V}{5} + \frac{Ni+Cu}{15} \qquad (1)$$

The necessity of applying preheat or postheat as well as the temperature depends not only on the C_{eq} but also on the expected diffusion hydrogen content in the weld metal and the geometrical characteristics of the weldments. To calculate the preheating temperature T_p [°C], the relationship according to Séferian can be used (eq. 2) The calculation has been determined for the diffusion hydrogen content and cooling rates typical for arc technologies). Therefore, the result of the calculation is approximate for the purpose of electron beam welding. The great advantage of electron beam welding is the reduction of hydrogen in the weld metal by the effect of the high vacuum during welding[4, 5].

$$T_P = 350\,.\sqrt{[C] - 0{,}25} \qquad (2)$$

Where the total carbon equivalent in steel C with thickness t [mm] is the sum of the chemical carbon equivalent C_{EC} and the thickness dependent equivalent C_h (Eq. 3 and 4).

$$C_{EC} = \frac{360\,.C + 40\,.(Mn + Cr) + 20\,.Ni + 28\,.Mo}{360} \qquad (3)$$

$$C_h = 0{,}005\; t\,.C_{EC} \qquad (4)$$

The objective of preheat is to provide a sufficiently long cooling time of the material to suppress martensitic transformation of the WM and HAZ. If the cooling rate is supercritical, martensitic transformation will occur in the areas heated above the austenitizing temperature, and the structure will be very hard, sensitive to hydrogen embrittlement. If the martensitic transformation termination temperature Mf is below 0 °C, the martensitic transformation does not take place completely and retained austenite may be present in the structure. Even the structure formed by the lower bainite does not provide sufficient toughness to prevent hydrogen-induced cracking. The prediction of the structure of WM and HAZ can be made with some approximation using the Time Temperature Transformation diagram – TTT (TTT diagram for steel W No. 1.7225) (fig. 1). If the temperature of WM or HAZ heated above A_{C1} and A_{C3} drops below 350 °C (M_s) in less than 9 seconds and martensitic transformation takes place. The resulting structure will consist of martensite and retained austenite[7, 9, 10, 11].

Prolonging the cooling time of the mentioned regions over 10 seconds will allow the bainitic transformation to take place partially. The resulting hardness of the structural components (lower bainite and martensite) will be approximately 600 HV. In order to achieve weld hardnesses below the prescribed 500 HV, it is necessary to extend the cooling time so that the temperature does not fall below 320 °C before about 100 s. Such cooling conditions should allow the formation of a structure consisting of 60 % bainite (upper) and a structural hardness below 500 HV [5, 6, 10].

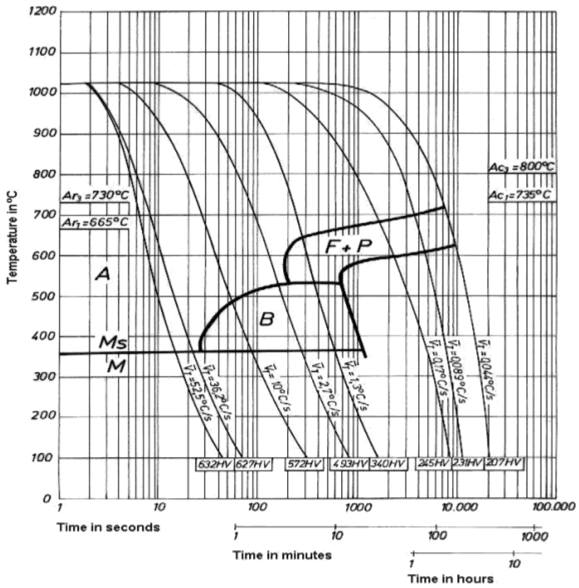

Fig. 1. TTT diagram of steel W. Nr. 1.7225

Source: online material datasheet – Steel W. Nr. 1.7225 –
https://steelselector.sij.si/steels_cct/vcmo140.html

Preheating parts before welding is complicated for several reasons. Preheating the part before welding outside the welding chamber requires handling and clamping the part at temperatures that can reach 350 °C. This also raises a problem from a safety point of view. A further complication in electron beam welding is the need to generate a vacuum in the welding chamber. Pumping the chamber to working pressure takes approximately 10 minutes in the case of the PZ EZ UNI 2G universal electron beam machine. During this time, the workpiece can cools down and therefore the temperature before welding may be lower than necessary. It would be necessary to increase preheat temperature of the piece by this temperature difference. The integration of any preheating method (flame, induction heating, electric resistance heating, etc.) is limited by the characteristics of the high vacuum environment, the contamination of the heating elements by metal vapours during the welding process, and the possible undesired influence of the electron beam by magnetic fields.The electron beam is a versatile heat source with a wide range of parameters and can therefore be effectively used as a preheating heat source. The advantage is the high vacuum environment and its protection of the weld joint and the entire surface of the component against oxidation. Since preheat is carried out in a chamber pumped to working pressure (less than 9.10^{-2} Pa), the welding process can follow immediately after the preheat process.

The electron beam power is directly proportional to the accelerating voltage U [kV] and the beam current I [mA], while the amount of heat Q [J] delivered to the body is approximately equal to the beam power P [W] and the beam exposure time t [s] (eq. 5). The electron energy transfer efficiency is close to 100 %. Losses due to incomplete absorption and scattering of electrons should be neglected for the simplicity.

$$Q = P_{EB} \, . t = U \, . I \, . t \qquad (5)$$

Tack welding and welding processes must also be included in the heat input.

The time $t_{preheat}$ [s] required to heat the weldment to the required temperature can be determined from the amount of heat input to the weldment during the preheating process by modifying Equation 7. However, the amount of heat input during tack welding or welding must also be taken into account. At the same time, the heat loss must also be taken into consideration. The high vacuum environment simplifies the calculation, since the losses due to the flow of the atmosphere around the weldment can be ignored and only the losses due to radiation and conduction to the jig can be taken into the calculation. The heat loss by radiation of the heated object can be quantified starting from the Stefan - Boltzmann law (eq. 6) for a grey body with emissivity ε = 0.8. Where $PS_{\_radiation}$ [W] the radiant heat power of a body with surface area S [m^2] heated to temperature T [K].

$$PS_{\_radiation} = \varepsilon \, . \sigma \, . T^4 . S \qquad (6)$$

The heat loss through the $PS_{\_conduction}$ [W] to the fixture represents the heat dissipation from the weldment and fixture to the rotary positioner and positioning system and can can be calculated from the eq. 7.

$$PS_{\_conduction} = \lambda \, . S \ \ . \frac{\Delta T}{l} \qquad (7)$$

2. MATERIALS AND METHODS

The main focus of the work was to handle the welding of a combination of selected types of difficult-to-weld Cr-Mo steels for hardening. The progress of the work has resulted in the experimental verification of the procedures on real samples of typical representatives for gear components. The main task was to determine the temperature conditions before and during the electron beam welding process, which will allow to achieve welded joints of the required quality. In the case of the necessity to use preheating, we proceeded to the use of the electron beam as a power source, with all the advantages it provides. Experiments of preheating and welding were carried out at the company PRVÁ ZVÁRAČSKÁ, a. s. (PZ a. s.) on the PZ EZ UNI 2G equipment. Metallographic analyses and hardness measurements of welded joints were carried out at the Accredited Laboratory of Metallography, Mechanical Testing and NDT at PZ a. s.

The company PRVÁ ZVÁRAČSKÁ a. s. has more than twenty years of history in the field of electron beam welding technology research and the supply of welding equipment for external customers. There are currently 9 welding complexes located in the laboratory of electron beam technologies. Of this number, there are 5 fully automated welding devices designed for highly productive EB welding of components of electric and hybrid cars, three electron beam welding devices for the realization of a wide range of welds for external customers and two universal welding devices for the research of electron beam welding technology and the realization of demanding welded joints for external customers.

Research on welding technology of selected two types of Cr-Mo steels was carried out on a modified electron beam welding device type PZ ELZA UNI 2G. The experimental workplace was arranged in such a way as to enable the realization of circumferential weld joints on samples of selected materials and selected configuration. The workstation positioning system allowed the movement of experimental samples in orthogonal linear x, y and z axes with fine control of position and speed. The rotary positioning system, which was superimposed on the 3D positioning system, allowed fine-tuning of the peripheral speed of the samples during the experiments. The experimental workplace has an internal volume of 3.02 m3 with internal dimensions of 1 300 x 1 500 x 1 550 mm, which represents sufficient space for the implementation of the expected experiments. The external appearance of the PZ EZ UNI 2G experimental workplace is shown in fig. 2.

Fig. 2. Experimental electron beam welding workplace for research on the welding of Cr-Mo steels

The workplace was equipped with two electron beam generation systems. Two atmospheric electron guns were placed on the top of the chamber and on the side wall of the chamber, one with a beam power of up to 7 kW and the other with a power of up to 30 kW. For the purposes of the experiments, an electron gun placed on top of the welding chamber was used. Its electron-optical system was configured for an output power of up to 7 kW at an accelerating voltage of 60 kV. This optical system enabled sharper focusing of the electron beam. A crystalline LaB_6 cathode with a diameter of 1.2 mm was used for electron emission. The cathode was indirectly heated by a bombardment of electrons from the back of the cathode. The output technical parameters of the subject electron beam generation system were as follows:

- Acceleration voltage: from 30 to 60 kV,
- range of beam power regulation: 30 W to 7 kW,
- working range of the welding current: from 1 to 120 mA,
- welding current stability: ± 1.2 %,
- stability of acceleration voltage: ± 1.0 %,
- voltage of the control electrode: 0-5 kV,
- cathode heating power: 20 – 100 W,

- focal current: 0.2 to 2 A,
- stability of the focal current: 0.5 %,
- deflection of the electron beam: up to ± 7 °. max.

The experimental workplace made it possible to adjust the beam to the weld joint using a CCD camera. The system is integrated in the electron gun and enables observation of the scene in the beam axis. From the point of view of electron beam diagnostics, the workplace is equipped to measure the transverse distribution of beam energy using the slit method with a Faraday cylinder. For comparison, the measured minimum diameter of the beam in the focal point at a distance of 300 mm from the focusing coil had a d4σ [1, 9] value of 0.4 mm at an accelerating voltage of 55 kV and a current of 100 mA. An integral part of the workplace is software for collecting and editing welding process parameters, which allows simultaneous recording of more than 15 process parameters with a sampling period of 1 to 10 ms. An example of recorded data is shown in fig. 3.

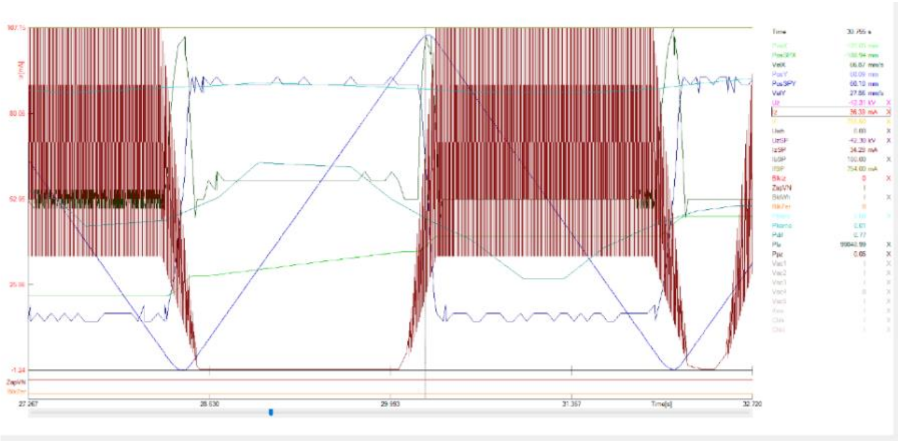

Fig. 3. Recording of welding process parameters in graphic form

The assembled experimental workplace enabled optimal positioning of the prepared experimental samples, precise adjustment of the electron beam to the weld joint, control of the parameters of the electron beam as well as the recording of selected parameters of the welding process.

2.1. Requirements for welds

The rotationally symmetrical body consists of three parts joined by two circumferential welds (fig. 4). The one weld, at a diameter of D 105 mm, joins the gear with external gearing (steel W. Nr. 1.7225) to the intermediate piece (steel W. Nr. 1.7325). The access to the weld located at diameter D 105 mm is complicated by the geometry of the part. The weld is located at the bottom of the groove with a width of 4.0 mm and a depth of 30 mm. The required depth of the weld is 6 mm.

The second weld is located on the outer circumference D 170 mm and joins the intermediate gear to the internal gear (steel W. No. 1.7225).. The required weld depth is min. 7 mm.

The weld quality acceptance criteria are at the level defined by STN EN ISO 13 919 - 1 grade D. The maximum permissible hardness in the welded joint area is 500 HV_{10}. A structure with a hardness lower than 500 HV_{10} will provide sufficient toughness for the weld joint to effectively resist hydrogen induced embrittlement.

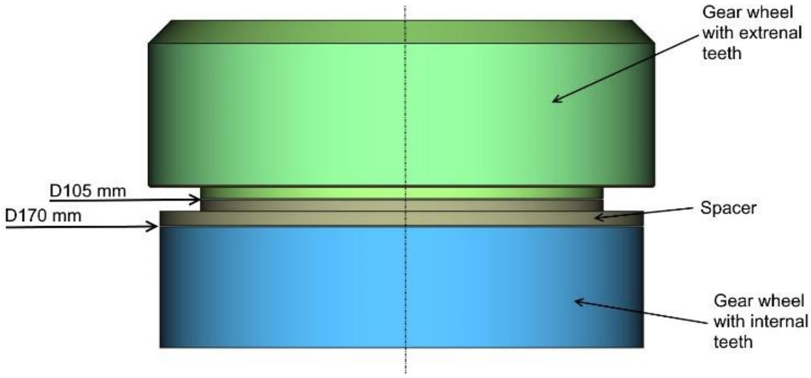

Fig. 4. Design of weldment and weld position and orientation of electron beam and placement of thermocouple during pre-heat process

2.2. Materials

2.2.1. Steel W. No. 1.7225 (42CrMo4)

This steel is one of the most widely used Cr-Mo steels used for quenching and surface hardening. It is used for heavily stressed machine parts requiring high strength and higher material toughness in the aerospace and automotive industries such as shafts, crankshafts, gears and fasteners, press tool components, guide rails, guides, etc. In the hardened state it reaches a strength of 1 100 MPa and hardness up to 61 HRC.

C (wt. %)	Si_{max} (wt. %)	Mn (wt. %)	P_{max} (wt. %)	S_{max} (wt. %)	Cr (wt. %)	Mo (wt. %)
0,38 – 0,45	0,40	0,60 – 0,90	0,035	0,035	0,90 – 1,20	0,15 – 0,30

Table 1. Nominal chemical composition of steel W. Nr. 1.7225

2.2.2. Steel W. No. 1.7325 (25MoCr4)

Mo-Cr steel used for cementing and refining with good strength at room and elevated temperature, good creep resistance. The maximum strength attainable after hardening is at the level of 1 250 to 1 370 MPa and hardness of 52 – 53 HRC.

C (wt. %)	Si_{max} (wt. %)	Mn (wt. %)	P_{max} (wt. %)	S_{max} (wt. %)	Cr (wt. %)	Mo (wt. %)
0,23 – 0,29	0,15 – 0,40	0,60 – 0,90	0,035	0,035	0,40 – 0,60	0,40 – 0,60

Table 2. Nominal chemical composition of steel W. Nr. 1.7325

2.3. Experimental procedures

The location of the electron beam during preheating was chosen in the weld area at the diameter D 105 mm. The location was chosen taking into account the geometry of the welded part. Since the weld is located in a massive part, which will ensure the accumulation and subsequent heat distribution without the risk of damage to the surface by local overheating. The preheating time must not be excessively long, but must ensure that sufficient heat is accumulated to reduce the steepness of the temperature gradients during cooling. The technological parameters of the preheating process have been chosen so that the material is melted as little as possible. The acceleration voltage was chosen to be the same as that used for welding to minimize the number of parameter changes and to limit possible operator errors and possible equipment failures. The electron beam current magnitude was chosen to be 70 mA. We minimized the amount of material to be melted by using high angular velocities ($70°.s^{-1}$). Simultaneously, during the preheating process, the electron beam is slightly defocused and dynamically deflected longitudinally with the weld axis. The deflection amplitude is ± 40 mm and the deflection frequency is 1.2 kHz. Transverse deflection cannot be used to increase the beam interaction area due to the 4 mm groove width. The parameters used for tack welding and welding are listed in table 3.

Process	**U [kV]**	**I_w [mA]**	**ω [$°.s^{-1}$]**	**I_f [mA]**
Tack weld (D 105 mm)	55	20	12	503
Tack weld (D 170 mm)	55	20	12	513
Weld (D 105 mm)	55	55	17	513
Weld (D 170 mm)	55	65	11	513

Table 3. Main technological parameters of electron beam tacking and welding processes

The temperature profile during preheats and welding was measured and recorded using an encapsulated K-type thermocouple. The thermocouple was positioned in the weld area No. 1 at a diameter D of 105 mm displaced 180° with respect to the electron beam (fig. 5). The purpose of the thermocouple was to measure the temperature of the preheated body.

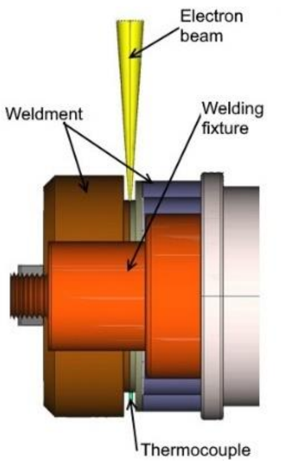

Fig. 5. Design of weldment and weld position and orientation of electron beam and placement of thermocouple during pre-heat process

The parameters required to weld with the required penetration were tuned on test specimens in the form of a hollow cylinder with a wall thickness corresponding to the prescribed weld penetration. Considering the chemical composition of the materials, we focused on slower welding speeds and adjusted the beam power accordingly. The process parameters for tack welding and welding are shown in table 3.

Three preheat temperatures (160; 200; and 350 °C) and one sample without preheat were welded. Preheating parameters were determined for the three different preheating modes according to the above-mentioned methodology. The calculated values of the preheating parameters taking into account the losses $PS_{\_radiation}$ and $PS_{\_conduction}$ are given in table 4.

$T_{preheat}$ [°C]	$Q_{preheat}$ [J]	$Q_{tack\ weld}$ [J]	$t_{preheat}$ [s]	$PS_{\_radiation}$ [W]	$PS_{\_conductio}$ [W]	$t_{preheat+losses}$ [s]
160	515 520	66 000	109	158	140	112
200	662 400	66 000	144	225	187	145
350	1 214 400	66 000	278	676	362	353

Table 3. Calculated approximate value of pre-heat time necessary for achieving required temperatures

3. RESULTS

The calculated values match the measured data quite well. It is possible to identify the action of the electron beam and the individual steps of the process quite accurately from the temperature profile (fig. 6).

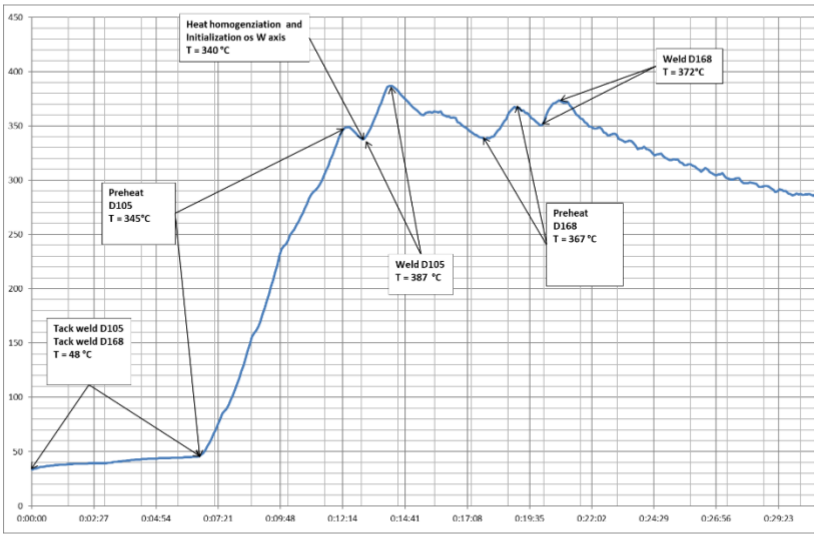

Fig. 6. Time course during whole processes of pre-heat, welding and cooling

The surface appearance of welded joints welded without and with preheating was similar, typically a narrow weld with a slight elevation. As the preheat temperature increased, the surface "colouration" due to oxidation intensified. Surface oxidation occurred when the welding chamber was aerated, as the temperature of the weldment exceeded 250 °C even 8 minutes after the weld was completed.

The structure of the parent material (PM) of all samples (welded without and with preheat) was similar and determined by the heat treatment of the gears before welding. The structure of the steel W. No. 1.7225 gears was formed by the decay structures of tempered martensite (fig. 7a). The spacer of steel W. No. 1.7325 did not undergo heat treatment and its structure formed by ferrite and pearlite is documented in fig. 7b. In the case of steel W. No. 1.7325 the measured PM hardness was in the range of 240 to 260 HV_{10} in all cases. Steel W. Nr. 1.7225, which underwent heat treatment before welding, showed a larger variance of the measured hardness values (250 to 300 HV_{10}). The variance in values was probably due to minor differences in conditions during heat treatment of the individual pieces.

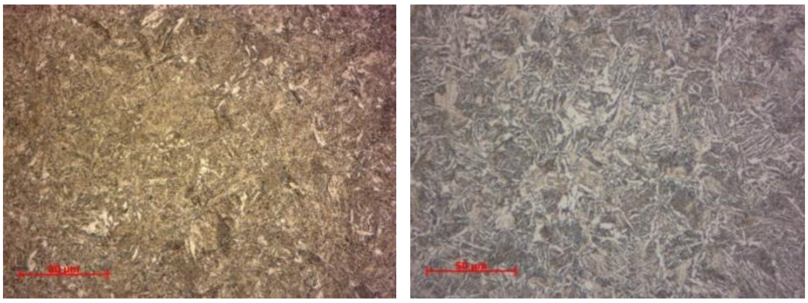

a b

Fig. 7. Structure of parent material a) steel W. Nr. 1.7225; b) steel W. Nr. 1.7325

3.1. Weld without preheat

The width of the weld welded without preheating was 0.8 mm, the HAZ was symmetrical and was approximately 1.2 to 1.3 mm for weld No. 1 located in the groove. In the case of weld No. 2 welded at a diameter D of 170 mm, the HAZ was asymmetrical, due to heat transfer. On the side with less heat sink, it was 2.5 mm wide. The WM was formed, due to the high cooling rate, by massive needles of martensite, retained austenite and lower bainite (fig. 8a). This corresponded to the measured hardness value. The highly heated HAZ (heated above the A_{C1} temperature) was formed, similarly to the weld metal, by a mixture of martensite, retained austenite and lower bainite see fig. 8b. Since it was not heated to as high temperature as the WM, grain coarsening did not occur to as great an extent. Hence, the structure is finer grained. The low-heated HAZ is formed by decay structures of tempered martensite with precipitation of fine carbides (fig. 8c). The highest hardness value measured was 608 HV_{10}. This value was measured in the TOO of steel W. No. 1.7325 of weld No. 1 at a diameter D of 105 mm. Other measurements in this area also exceeded the value of 600 HV_{10}. The measured hardness of the WM was in the range of 586 to 590 HV_{10} for weld No. 1. The WM of weld No. 2 showed similar values of 578 to 599 HV_{10}. The hardness of HAZ steel W. No. 1.7225 reached a level of 400 to 450 HV_{10}. The measured hardness values of the WM and HAZ confirm the structures identified by light microscopy. Weld No. 2, at a diameter D of 170 mm, showed a similar pattern of hardness values as weld No. 1.

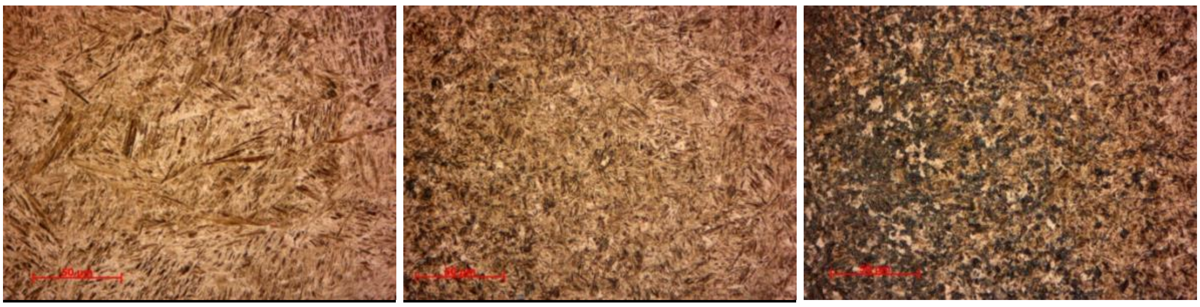

a b c

Fig. 8. Microstructure of joints welded without pre-heat a) weld metal, b) coarse grain HAZ, c) fine grain HAZ

3.2. Weld with preheat 160 °C

The HAZ widths were similar to the welding without preheat and their widths were around 1.2 mm. The preheating temperature was not sufficient and the cooling rate of the weld metal was still relatively high. Therefore, the WM is formed by a mixture of martensite, retained austenite and lower bainite (fig. 9a). The structures in the HAZ were similar to those observed for the welds without preheating (fig. 9b and 9c). The application of preheat resulted in a slightly coarser structure compared to the weld welded without preheating. However, preheating the weld to 160 °C did not prevent the formation of hard structural components. The highest hardness value measured was 637 HV_{10}. This value was measured in HAZ steel W. No. 1.7325 of weld No. 1 at a diameter D of 105 mm. The other two measurements in this area exceeded the value of 550 HV_{10}. The measured hardness of the weld metal reached a maximum value of 522 HV_{10}. The hardness of HAZ steel W. No. 1.7225 was 487 HV_{10}. The measured WM hardness and HAZ hardness values confirm the structures identified by light microscopy. Weld No. 2 on average did not show such high hardness values compared to weld No. 1. The maximum measured value was 559 HV_{10} (HAZ - steel W. No. 1.7325), the measured hardness of the weld metal was at 544 HV_{10}.

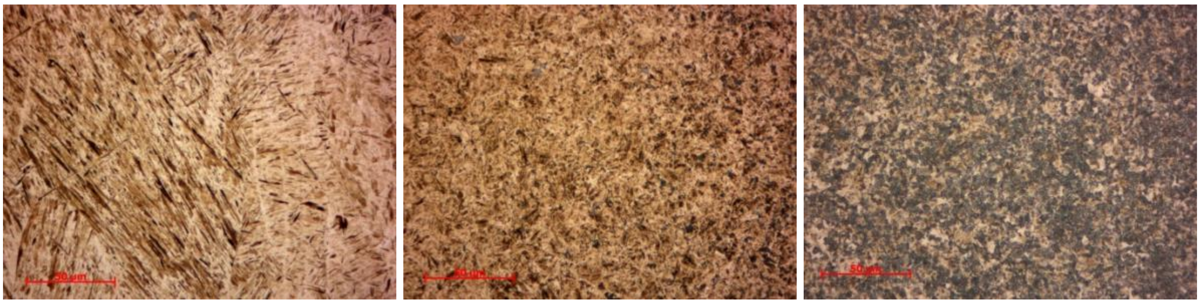

a b c

Fig. 9. Microstructure of joints welded with pre-heat temperature 160 °C a) weld metal, b) coarse grain HAZ, c) fine grain HAZ

3.3. Weld with preheat 200 °C

The increased preheating temperature resulted in an increase in HAZ width to 1.4 mm in the case of the 200 °C preheat. Another manifestation of the lower cooling rate was an increase in the proportion of bainite in the weld metal structure (fig. 10a). The highly heated part of the HAZ (fig. 10b) was formed by the bainitic structure. And in the low-heated region of HAZ, decay structures were again observed (fig. 10c). In the case of welds made with 200 °C preheat, the change of the structure was positively reflected in the decrease of hardness. Nevertheless, the measured hardnesses exceeded the maximum permissible values. Specifically for weld joint No. 1 in HAZ steel W. No. 1.7325, values of 572 and 566 HV_{10} were measured. In HAZ steel W. No. 1.7225, the measured hardness values were in compliance with the requirements (339 and 401 HV_{10}). The hardness values of the WM reached a maximum value of 573 HV_{10}. The maximum measured hardness values were 535 and 551 HV_{10} (WM), and for HAZ it was 331 to 544 HV_{10}.

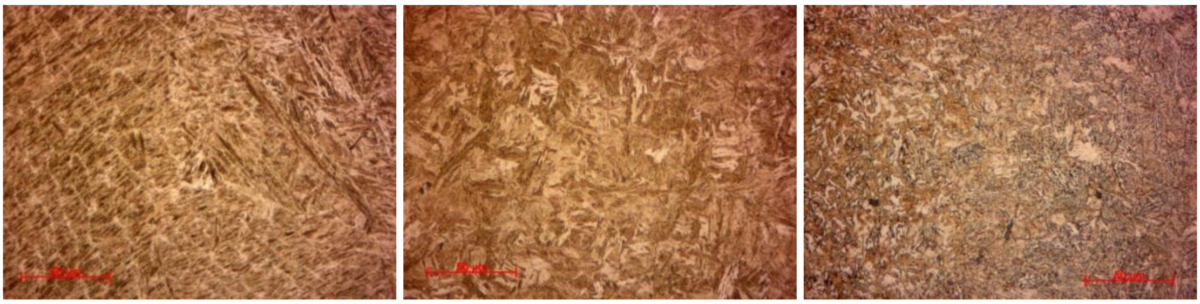

a b c

Fig. 10. Microstructure of joints welded with pre-heat temperature 200 °C a) weld metal, b) coarse grain HAZ, c) fine grain HAZ

3.4. Weld with preheat 350 °C

The HAZ width reached a value of over 1.6 mm. Preheating the weld metal prolonged the cooling time so that no martensitic transformation took place as the weld metal cooled. In the WM structure, we can observe upper bainite, ferrite and pearlite (fig. 11a). The structure of the highly heated part of HAZ is formed by a mixture of upper bainite ferrite and pearlite (fig. 11b). The low-heated part of HAZ is formed by decay structures, with an increased proportion of ferrite (fig. 11c).

The measured hardness profile fully corresponds to the observed structure. In the case of weld No. 1, the hardness of the WM ranges from 289 to 343 HV_{10}. The hardnesses detected in the HAZ do not exceed 347 HV_{10}. Similar results were found for weld No. 2, namely weld metal hardnesses of 328 to 341 HV_{10}. The HAZ showed a slightly larger variance of 252 to 344 HV_{10}.

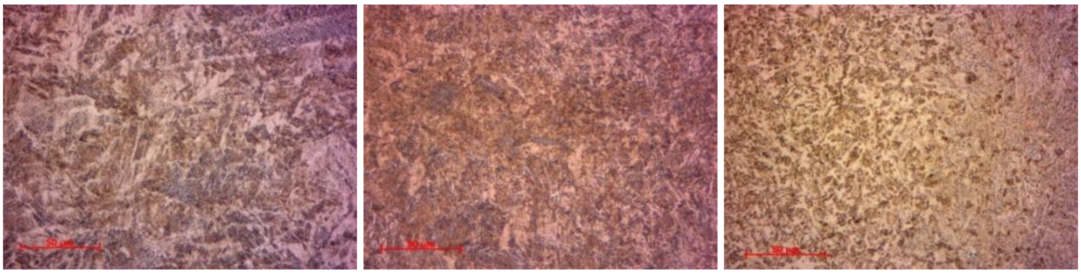

a b c

Fig. 11. Microstructure of joints welded with pre-heat temperature 350 °C a) weld metal, b) coarse grain HAZ, c) fine grain HAZ

4. CONCLUSIONS

Electron beam welding does not allow to influence the carbon equivalent of the weld metal, thereby suppressing the susceptibility to cold cracking to some extent. Therefore, a preheat or postheat mode is required to eliminate cold cracking. A dynamically deflected and defocused electron beam can be used as a heat source without any modification to the device.

Due to the shape of the part, it was not possible to use other than beam technology for welding. The biggest limitation was the positioning on the D 105 diameter in a groove with a width of 4 mm and a depth of 30 mm.

Due to the fact that the largest volume of material is localized in the area of weld No. 1 (gear with external teeth), we chose weld No. 1 in particular as the electron beam heating location. In order to avoid unwanted excessive melting of the material during preheating, it was necessary to use high speed ($\omega = 70°.s^{-1}$) and dynamic deflection of the beam with an amplitude of ± 40 mm and a frequency of 1.2 kHz.

Approximate calculations made it possible to determine the preheating conditions of the weldments and provided relevant results, which were confirmed by temperature measurements using a thermocouple.

Regardless of the preheating temperature used, the welds had a similar appearance and the weld depth corresponded to the selected electron beam power. The preheat temperature had no significant effect on the weld depth and width.

The preheat temperatures of the welds understandably had an effect on the structure of the welded joints and also on the hardnesses achieved. Similarly, preheating also had an effect on the width.

The welding procedure without the application of preheat led to the formation of a martensitic structure of the weld metal, which was also confirmed by metallographic analysis and hardness measurements across the welded joint. The maximum measured hardness value exceeded 600 HV_{10}. The formation of the hard martensitic structure resulted in the formation of cold cracks in the weld joint during cooling.

In the case of steels with conditional weldability designed for hardening, it is necessary to apply special temperature regimes. Neither the low diffusible hydrogen content of the weld metal nor the small amount of heat input and therefore the lower induced stresses prevented the formation of cold cracks.

Preheating temperatures of 160 °C and 200 °C, were accompanied by a small decrease in hardness, but were not sufficient to suppress martensitic transformation and resulted in only partial grain coarsening. The weld metal structure and the high-heat HAZ consisted of a mixture of martensite and lower bainite, the hardness of the structure decreased only very slightly and, apart from the susceptibility to cold cracks, did not meet the requirements for a maximum value of up to 500 HV_{10}.

The best results in terms of structure and hardness were obtained by samples welded with preheat of 350 °C. Virtually no martensite was observed in the structure of the weld metal. The hardness in the weld metal and HAZ was at a suitable level (safely below the maximum prescribed value) and the structure possessed sufficient toughness to successfully resist cold cracks. This created the way for the design and successful testing of industrial cadence welding of small series of gear components made from a combination of Cr-Mo steels.

ACKNOWLEDGMENTS

This work was supported by the Slovak Research and Development Agency under contract No. APVV-APVV -20- 0100, and by Ministry of Education, Science, Research and Sport of the Slovak Republic within the call Stimuly 2018 based on Contract Reg. No. 1227/2018.

REFERENCES

1. von Dobeneck D., Loewer Th, 2005, *Economizing Electron Beam Welding - Recent Developments and Future Trends,* Proceedings from the International Conference, Welding Technology - Technology for Development of EU Industry
2. Hrivnak, I 1992, *Theory of weldability of metals and alloys*, Elsevier, Amsterdam, ISBN 0-444-98707-X
3. Lippold, JC, 2015, *Welding metallurgy and weldability*, Wiley & Sons, New Jersey, ISBN 978-118-23070-1
4. Messler R Jr., 2004, *Principles of welding - Processes, physics, chemistry and metallurgy*, Wiley-Vich Verlag, New York, ISBN 978-0-471-25376-1
5. Kearns, WH, 1997, *Welding Handbook Vol. 4 metals and their weldability,* 7th Ed, AWS, Miami, ISBN 0-87171-218-0
6. Schultz H, 2004, *Electron beam welding,* Abington Publishing, Cambridge, ISBN 1-85573-050-2
7. Meleka AH, 1971, *Electron-beam welding: principles and practice,* McGraw-Hill, London, ISBN 978-0070942189
8. Halliday D., Resnick R., Walker J.: *Fundamentals of physics*, 10th Ed, 5 John Wiley & Sons, USA, ISBN 978-1-118-23061-9
9. Kolenič F, Kováč Ľ, Sekerka R, Faragula P, 2019, *Modular Design of Productive Electron Beam Welding Machines*, Paton Welding Journal, No.03, 2019 pp, 34-41, ISSN 0957-798X, DOI: https://doi.org/10.15407/tpwj2019.03.06
10. McKenzie DS., Totten GE, 2006, *Analytical Characterization of aluminum, steel and superalloys,* CRC Press, New York, ISBN 0-8247-5843-9
11. Bhadeshia HKDH, Honeycombe RWK, 2006, *Steels microstructure and properties,* 3rd Ed, Elsevier, Oxford, 2006, ISBN 978-0-750-68084-4

12. Online material datasheet – Steel W. Nr. 1.7225 – https://steelselector.sij.si/steels_cct/vcmo140.html, cit. 25. 07. 2024